

Spontaneous rotating vortex rings in a parametrically driven polariton fluid

J. O. HAMP^{1,2} (a), A. K. BALIN^{1,3} (b), F. M. MARCHETTI⁴, D. SANVITTO⁵ and M. H. SZYMAŃSKA^{1,6} (c)

¹ *Department of Physics, University of Warwick, Coventry, CV4 7AL, UK*

² *TCM Group, Cavendish Laboratory, University of Cambridge, Cambridge, CB3 0HE, UK*

³ *Rudolf Peierls Centre for Theoretical Physics, University of Oxford, Oxford, OX1 3NP, UK*

⁴ *Departamento de Física Teórica de la Materia Condensada & Condensed Matter Physics Center (IFIMAC), Universidad Autónoma de Madrid, Madrid 28049, Spain*

⁵ *NNL, Istituto Nanoscienze-CNR, Via Arnesano, 73100 Lecce, Italy*

⁶ *Department of Physics and Astronomy, University College London, Gower Street, London, WC1E 6BT, UK*

PACS 71.36.+c – Polaritons (including photon-photon and photon-magnon interactions)

PACS 03.75.Lm – Tunneling, Josephson effect, Bose-Einstein condensates in periodic potentials, solitons, vortices, and topological excitations

PACS 42.65.Yj – Optical parametric oscillators and amplifiers

Abstract – We present the theoretical prediction of spontaneous rotating vortex rings in a parametrically driven quantum fluid of polaritons – coherent superpositions of coupled quantum well excitons and microcavity photons. These rings arise not only in the absence of any rotating drive, but also in the absence of a trapping potential, in a model known to map quantitatively to experiments. We begin by proposing a novel parametric pumping scheme for polaritons, with circular symmetry and radial currents, and characterize the resulting nonequilibrium condensate. We show that the system is unstable to spontaneous breaking of circular symmetry via a modulational instability, following which a vortex ring with large net angular momentum emerges, rotating in one of two topologically distinct states. Such rings are robust and carry distinctive experimental signatures, and so they could find applications in the new generation of polaritonic devices.

Introduction. – Macroscopically coherent quantum fluids exhibit excitations in the form of quantized vortices – topological defects in the order parameter describing the condensed phase. The ubiquity of quantized vortices has become increasingly apparent since their prediction in superfluids some decades ago [1], and they are now known to play a key role in the physics of equilibrium systems such as ultracold atomic gases, liquid helium, and type-II superconductors [2].

More recently, condensation of bosonic quasiparticles, such as microcavity polaritons [3], has been observed. Polaritons are coherent superpositions of coupled quantum well excitons and microcavity photons. They have a finite lifetime, so their condensation is intrinsically nonequilibrium:

continuous repopulation from an external source is necessary to balance photonic losses from the cavity. In the optical parametric oscillator (OPO) regime [4, 5], polaritons are resonantly injected into a pump state by a coherent laser field, before undergoing parametric scattering to signal and idler states. The sum of the phases of the signal and idler is locked by the pump, but their relative phase is otherwise free, and any explicit choice by the system breaks U(1) gauge symmetry. In this sense, though out-of-equilibrium, the system can be thought of as a quantum condensate in the same way as an equilibrium Bose-Einstein condensate – both are characterized by the appearance of a Goldstone mode [6].

Parametrically driven polariton fluids have been shown to have nonequilibrium superfluid properties [7, 8], and exhibit complex and varied behavior such as quantized vortices and persistent currents [9–11]. Under certain ex-

(a) E-mail: joh28@cam.ac.uk

(b) E-mail: andrew.balin@physics.ox.ac.uk

(c) E-mail: m.szymanska@ucl.ac.uk

ternal perturbations, quantized vortices can form nontrivial patterned structures: for example, in ultracold atomic gases under a rotating drive, or type-II superconductors in an external magnetic field [2]. However, the appearance of vortices, and their subsequent pattern formation, is not expected to occur spontaneously, without an external injection of angular momentum of some kind.

In this letter, we present the theoretical prediction of spontaneous vortex rings in a nonequilibrium polariton fluid driven in the parametric regime. These vortex rings have nonzero net angular momentum, and appear due to the strong driving and dissipation in the system – not only in the absence of any rotating drive, but also in the absence of a trapping potential.

We begin by proposing a novel and experimentally viable parametric pumping scheme for polaritons, with circular symmetry and radial currents. We then characterize the resulting circularly-symmetric condensate. In many cases the system is unstable to spontaneous breaking of circular symmetry via a modulational instability, and undergoes the formation of vortex rings in the absence of any rotating drive. These rings have nonzero net angular momentum and rotate in one of two degenerate but topologically distinct states of opposite chirality. Their presence leads to side bands in the photoluminescence spectrum of the system [12], which constitutes an accessible experimental signature of such a ring, in addition to possible direct imaging with time-resolved techniques.

These are the first examples of spontaneous vortex rings in parametrically driven polariton fluids, and find their natural place in the wider framework of pattern formation in out-of-equilibrium systems [13]. They are fundamentally different from the spontaneous vortex-antivortex rings recently observed in other studies of polaritons under different pumping schemes [14–16], in that here all vortices have the same vorticity, and correspondingly the rings carry nonzero net angular momentum. Spontaneous vortex arrays with nonzero net angular momentum had been predicted to arise [17] in a simplified model of an incoherently-pumped polariton condensate, but there they necessitated an harmonic trapping potential. Our rings, beyond being the first examples of spontaneous vortex rings of this type in a parametrically driven polariton fluid, provide great encouragement for the first experimental observation in any polariton system, since they carry distinctive experimental signatures, and dispense with the need for harmonic trapping potentials [18]. Moreover, they occur in a model which is known to map quantitatively to experimental systems, unlike those of incoherently-pumped systems, where the roles of the excitonic reservoir and thermalization are not well understood. Due to their controllable, topologically robust nature, with large angular momentum, they have the potential to find applications in the new generation of polaritonic devices [19–21].

Methods. – Semiconductor microcavity polaritons in the parametrically driven (OPO) regime are known to

be well described by a generalized Gross-Pitaevskii (GP) equation [22] that is derivable as the mean-field limit of a microscopic theory where exciton-exciton and exciton-photon interactions, and the pumping and decay processes, are all treated explicitly. The details are reviewed in Ref. [23] and references therein.

The coupled exciton (X) and cavity photon (C) fields $\psi_{X,C}(\mathbf{r}, t)$ decay with rates $\kappa_{X,C}$ respectively, and mix with strength $\Omega_R/2$, where Ω_R is the Rabi splitting between the upper (UP) and lower (LP) branches of the polariton dispersion at zero detuning. The excitonic dispersion ω_X is taken to be constant ω_X^0 , and the photonic dispersion is given by $\omega_C = \omega_C^0 - \frac{\nabla^2}{2m_C}$, where m_C is the cavity photon mass. The generalized GP equation is then (we set $\hbar = 1$ throughout):

$$i\partial_t \begin{pmatrix} \psi_X \\ \psi_C \end{pmatrix} = \begin{pmatrix} 0 \\ F_p \end{pmatrix} + \begin{pmatrix} \omega_X - i\kappa_X + g_X|\psi_X|^2 & \Omega_R/2 \\ \Omega_R/2 & \omega_C - i\kappa_C \end{pmatrix} \begin{pmatrix} \psi_X \\ \psi_C \end{pmatrix}, \quad (1)$$

where g_X is the strength of the exciton-exciton interaction and $F_p(\mathbf{r}, t)$ is the pump field. The traditional OPO system is driven by a coherent continuous-wave pump, $F_p(\mathbf{r}, t) = \mathcal{F}_p(r) e^{i(\mathbf{k}_p \cdot \mathbf{r} - \omega_p t)}$, with \mathbf{k}_p fixed in one particular direction (e.g. the x -direction), and a smoothed top-hat or Gaussian spatial profile $\mathcal{F}_p(r)$ of strength f_p and full width at half-maximum (FWHM) σ_p . The fields $\psi_{X,C}$ and pump strength f_p can be rescaled by $\sqrt{\Omega_R/(2g_X)}$ so that the exciton interaction strength g_X is unity. In the present work we use $m_C = 2 \times 10^{-5} m_e$, $\Omega_R = 4.4$ meV (both typical of GaAs-based microcavities), and zero detuning.

Equation (1) describes a system that exhibits rich and complex phenomena arising from the subtle interplay between pumping, decay, nonlinearity, and the system being finite size. It is well known that for finite size pump profiles, no approximate analytic analysis that captures the OPO physics – including the instability to spontaneous vortex formation – is possible [10, 22, 24]. We proceed by solving Eq. (1) via a fifth-order adaptive-step Runge-Kutta algorithm for a system of size $120 \times 120 \mu\text{m}$ discretized onto $2^8 \times 2^8$ points in space. The pump is chosen to have wave vector $|\mathbf{k}_p| = 1.6 \mu\text{m}^{-1}$ and energy $\omega_p = -0.44$ meV, in resonance with the point of inflection of the LP dispersion branch after blueshifting [25] of the polariton dispersion.

Pumping scheme. – We build upon previous theoretical work in polariton fluids [26] by proposing a new parametric pumping scheme $F_p(\mathbf{r}, t)$. We use $F_p(\mathbf{r}, t) = \mathcal{F}_p(r) e^{i(k_p r - \omega_p t)}$, and a smoothed top-hat spatial profile $\mathcal{F}_p(r)$. This pumping configuration corresponds to a circularly symmetric profile, with constant radial currents given by $|\mathbf{k}_p| \hat{\mathbf{r}}$. The absolute value of the Fourier transform (zeroth order Hankel transform) of the pump field in two-dimensional momentum space $|F_p(\mathbf{k})|$ is shown in

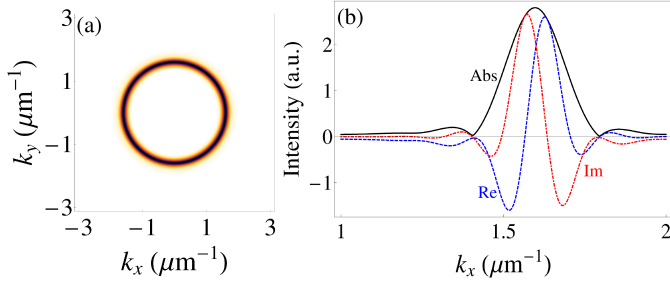


Fig. 1: (Colour on-line) External pump used to drive the system in the OPO regime. In real space the pump is given by $F_p(\mathbf{r}, t) = \mathcal{F}_p(r) e^{i(k_p r - \omega_p t)}$, with a smoothed top-hat profile $\mathcal{F}_p(r)$, i.e., constant radial currents of strength $|\mathbf{k}_p|$. (a) The absolute value of the Fourier transform of the pump field, in two-dimensional momentum space. The pump constitutes a ring of radius $|\mathbf{k}_p|$. (b) A cut along $k_y = 0$, showing the details of the ring profile in momentum space: absolute value, and real and imaginary parts.

Fig. 1 (a); it is a ring of radius $|\mathbf{k}_p|$. The profile of the ring is shown in detail in a cut along $k_y = 0$ in Fig. 1 (b), along with the real and imaginary parts. This pumping scheme could be realized in experiments with the aid of an axicon lens, or engineered using the phase of the laser pump, and a spatial light modulator. It leads to the generation of an OPO state that is circularly symmetric both in real and in momentum space.

However, in order to investigate the dynamical stability of the steady-state symmetric system, a small perturbation has to be added. We use a weak probe field in resonance with the signal mode, but any other weak symmetry-breaking perturbation would work equally well. In what follows we only consider the photonic component of the polariton field since it is the quantity measured in experiments.

Results. – The full photoluminescence spectrum of the symmetric system with pump spot size $\sigma_p = 35 \mu\text{m}$ is shown in Fig. 2 (a) (along $k_y = 0$). The generation of OPO is evidenced by the presence of signal and idler states to which polaritons injected at the pump state parametrically scatter, the signal lying at low momentum and energy, and the idler at high momentum and energy¹. The total photonic emission in momentum space $|\psi_C(\mathbf{k})|$ of the same system can be seen in Fig. 2 (b), as a cut along $k_y = 0$. Again, the macroscopic populations of the pump (at $|\mathbf{k}_p| = 1.6 \mu\text{m}^{-1}$), signal (at $|\mathbf{k}_s| \sim 0$) and idler (at $|\mathbf{k}_i| \sim 2|\mathbf{k}_p|$) states are visible. We are interested in the behaviour of the signal mode population, which we obtain by filtering in energy or momentum, as is done in experiments. The idler has a conjugate behaviour to the signal (i.e., if vortices appear in the signal, antivortices will appear in the idler). The dashed lines in Fig. 2 (b) represent

¹The idler state is weak, and especially so in our system since it lies on a ring of large radius in two-dimensional momentum space, and is therefore correspondingly diluted in any one-dimensional cut.

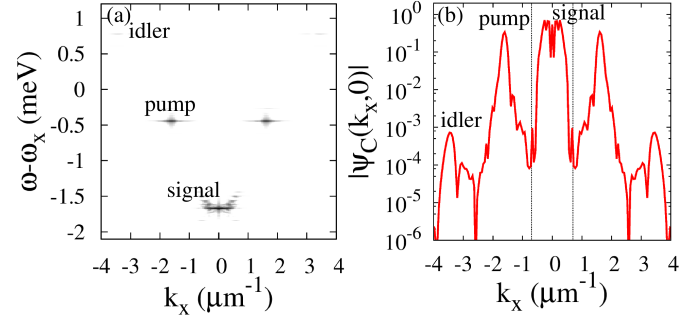


Fig. 2: (Colour on-line) (a) The full photoluminescence spectrum of the symmetric OPO system with $\sigma_p = 35 \mu\text{m}$, along $k_y = 0$. Polaritons are injected coherently into the pump state, and scatter parametrically into the signal and idler states. The intensity scale is logarithmic. (b) The momentum population of the symmetric system, $|\psi_C(\mathbf{k})|$, along $k_y = 0$. The strong occupations of the pump, signal, and idler modes as created by the OPO process can be clearly seen. Each can be obtained individually by filtering in a suitable window in momentum. The dashed lines indicate the window in which we filter to obtain the signal mode.

the window of $\pm 0.7 \mu\text{m}^{-1}$ around zero momentum which we use to filter out the the signal mode and obtain the signal field in real space $|\psi_C^s(\mathbf{r}, t)| e^{i\phi_C^s(\mathbf{r}, t)}$, where $\phi_C^s(\mathbf{r}, t)$ is the phase of the signal wave function.

The parametric scattering process occurs (‘switches on’) for certain ranges of detunings and pump momenta [25], only above some threshold pump strength f_p^{th} . We find the signal mode population to appear at $f_p \equiv f_p^{\text{th}}$ and increase above threshold up to some maximum value, before beginning to disappear (‘switching off’) at around $f_p = 1.6 f_p^{\text{th}}$. The maximum total signal intensity occurs for a pump strength of around $f_p = 1.5 f_p^{\text{th}}$. However, the shape of the signal in real space generally becomes more complicated and less uniform on increasing f_p too far above threshold, and after symmetry breaking, the time evolution is not stable. The regime slightly above threshold is where interesting behavior has been observed in previous work [10], and it is also the regime in which we observe steady-state vortex ring solutions. We observe vortex rings for $1.1 \leq f_p/f_p^{\text{th}} \leq 1.25$, and in the following we use $f_p = 1.2 f_p^{\text{th}}$ unless stated otherwise.

The photonic signal emission in real space $|\psi_C^s(\mathbf{r})|$ of the symmetric system with $\sigma_p = 35 \mu\text{m}$ and $\sigma_p = 46 \mu\text{m}$, can be seen in Figs. 3 (a) and (c), respectively. Superimposed are the supercurrents $\mathbf{j}(\mathbf{r}) \equiv |\psi_C^s|^2 \nabla \phi_C^s(\mathbf{r})$, which result from the interplay of spatially non-uniform pumping and decay. The small but dominant (radial) signal currents at nonzero $k = 0.25 \mu\text{m}^{-1}$ have been subtracted to reveal the more complex underlying steady-state current structure which moves particles from gain- to loss-dominated regions. There are sharp changes in the density profile of the condensate, and at the border of higher-and lower-density regions, discontinuities in the direction of the un-

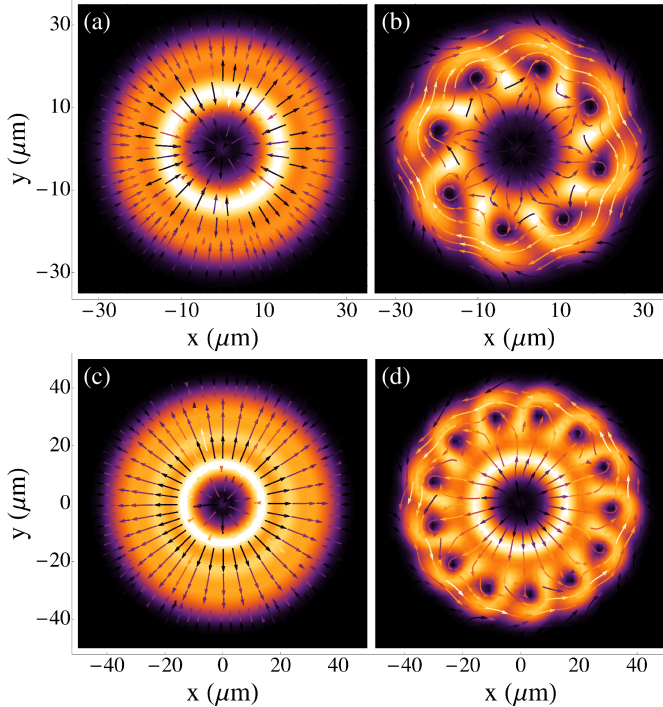


Fig. 3: (Colour on-line) The photonic component of the signal mode population of the system in real space $|\psi_C^s(\mathbf{r})|$. (a), (b): With $\sigma_p = 35 \mu\text{m}$. (a) In the absence of a vortex ring (before symmetry breaking). (b) In the presence of an 8-(anti)vortex ring. (c), (d): With $\sigma_p = 46 \mu\text{m}$. (c) In the absence of a vortex ring (before symmetry breaking). (d) In the presence of a 13-vortex ring. Superimposed are the supercurrents $\mathbf{j}(\mathbf{r})$. In the symmetric cases, the dominant signal current at small nonzero momentum has been subtracted to reveal the more complex underlying currents.

derlying currents. The pump state population is uniform and homogeneous throughout, as directly imposed by the top-hat spatial profile of the pump field, with strong currents directed radially outwards. It is not significantly modified by the presence of vortices in the signal and idler.

Once the system has evolved to a steady-state regime with balanced pumping and decay, we examine dynamical stability by adding a small perturbation. For this we add a Gaussian probe $F_p(\mathbf{r}, t) \rightarrow F_p(\mathbf{r}, t) + F_{pb}(\mathbf{r}, t)$, resonant with the signal mode but of much smaller dimensions ($\sigma_{pb} \sim 3 \mu\text{m}$), 10^{-3} times weaker than the pump, positioned such that $\mathbf{r} \times \mathbf{k}_{pb} = 0$, so as not to impose a preferred direction of symmetry breaking. The strength of the perturbation influences the transitory regime but has no bearing on the final solution. The discontinuities in the underlying current direction in the symmetric system correspond to polaritons travelling with smaller or larger velocities relative to the average. The presence of such radial counter-propagating currents, due to the strong driving, decay, and nonlinearity, means that system is dynamically unstable. This can be understood as similar to the situation in other nonlinear systems, such as water waves

approaching a shore, where the dispersion of the waves eventually leads to an instability.

Following the perturbation, vortices enter the condensate and stabilize there in an ordered ring. The ring can be formed of either vortices or antivortices and rotates clockwise or anticlockwise (respectively). However, neither rotation direction is preferred energetically – thus, the explicit choice made by the system spontaneously breaks circular symmetry. The physical mechanism of vortex ring formation is fundamentally spontaneous, however, in experiments, symmetry would be broken explicitly, e.g., by any small in-plane asymmetry of the cavity field. In the simulations, the direction of rotation can be controlled if desired, by breaking the symmetry explicitly in a particular direction, e.g., by imparting some momentum in that directions. However, if a noise perturbation is used that does not explicitly prefer any rotation direction, then for the same parameters but different noise realizations, the system will rotate sometimes left, sometimes right. In the presence of the vortex ring, the unstable radial counter-propagating currents are eliminated, and the flow of the condensate is controlled by the vortex ring. These vortex ring solutions are dynamically stable to noise or additional small perturbations, and we simulate the dynamics for very long times, ~ 15 ns.

An example of a steady-state vortex ring can be seen in Fig. 3 (b), with the supercurrents $\mathbf{j}(\mathbf{r})$ superimposed. The system is the same as that in Fig. 3 (a). The condensate contains 8 antivortices and rotates anticlockwise as a rigid body with angular frequency $\Omega = 9.91$ GHz. In the presence of the vortex ring, taking into account the currents in the whole signal state, there are no longer discontinuous changes in the current direction throughout the condensate as in the symmetric case (see Fig. 3, (a); (c)), and the vortex ring dominates the currents in the system. This 8-vortex ring solution is robust to varying σ_p and f_p by up to around $\pm 5\%$. When increasing (decreasing) σ_p by more than this, rings with greater (fewer) numbers of vortices can be generated, such as the 13-vortex ring in Fig. 3 (d), using a 30% larger pump spot size (the same system as in Fig. 3 (c)). This is due to the fact that vortices are organized such that their separation is set by the healing length, which is approximately constant, so that a larger condensate can support more vortices. Outside the window of $1.1 \leq f_p/f_p^{\text{th}} \leq 1.25$, however, the symmetry-broken system is unstable: vortices drift in and out of the condensate without ordering on the longest timescales we can simulate for. This is analogous to the lack of a steady-state for other effects in previous simulations of the OPO system [10]. However, if the pump is strong ($f_p \gtrsim 1.5$ over a range of σ_p values), and the signal population comparatively uniform, then the circularly symmetric solution is dynamically stable and no symmetry breaking occurs; this corresponds to when the condensate is at its most dense.

The appearance of the vortex ring can be understood as being due to a modulational instability of the symmetric system: in general, pumping and decay causes the fre-

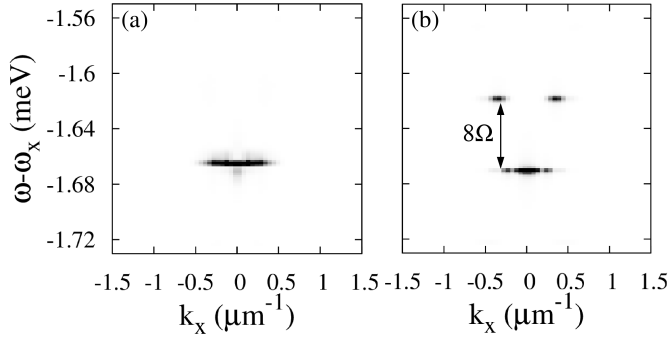


Fig. 4: (Colour on-line) The photoluminescence of the system close to the signal mode with $\sigma_p = 35 \mu\text{m}$, along $k_y = 0$. (a) In the absence of a ring (before symmetry breaking). (b) In the presence of an 8-(anti)vortex ring. In both cases the signal mode population around $k = 0$ can be seen. In the presence of the ring two additional side-bands, arising from rotation of the condensate, appear $\Delta E = 8\Omega$ above the signal energy.

quencies of a stationary, homogeneous state to acquire an imaginary part, leading to growth of the associated high angular momentum modes, and vortex nucleation [17, 27]. As such, our rings are predicted [12] to give rise to side bands in the photoluminescence spectrum, shifted in energy away from the condensate mode by $\Delta E = n\Omega$, where n is the number of vortices in the ring. The photoluminescence spectrum near the signal (along $k_y = 0$) of the system corresponding to Fig. 3 (a) is shown in Fig. 4 (a). The signal population can be seen around $k = 0$, $\omega - \omega_x = -1.67$ meV. The spectrum of the same system in the presence of an 8-vortex ring (Fig. 2 (b)) is shown in Fig. 4 (b). Two side bands lying above the signal state can be clearly seen. The energy shift ΔE of the side bands relative to the signal state is found to be 0.051 ± 0.002 meV, in very good agreement with the theoretical value of $8\Omega = 0.052$ meV. We find similarly good agreement in the case of rings with different numbers of vortices. For example, for a 12-vortex ring solution, we find the frequency of rotation to be $\Omega = 8.10$ GHz, giving a theoretical energy shift of $12\Omega = 0.064$ meV, and we observe the side bands to be shifted by 0.064 ± 0.002 meV away from the signal state. Based on our simulations, we believe that the vortex ring could be directly imaged, and its rotation measured, using state-of-the-art time-resolved techniques. For example, for a 8-vortex ring with $\sigma_p = 35 \mu\text{m}$ we predict a period of rotation of 634 ps, whilst for a 12-vortex ring with $\sigma_p = 43.5 \mu\text{m}$ we predict 776 ps, which should be long enough to allow direct imaging. However, for experiments which rely upon time-integrated measurements of photonic emission, direct observation of rotating vortex rings may be more difficult. The presence of side bands in the photoluminescence spectrum provides an alternative experimental signature of such a ring. Another possible method of directly imaging a rotating vortex ring in experiments using time-integrated measurements is via the defocused homodyne imaging scheme discussed in Ref. [27],

which exploits the presence of the side bands in the spectrum.

Conclusion. – We have presented the theoretical prediction of spontaneous rotating vortex ring formation in a parametrically driven polariton fluid. This has been achieved by proposing a novel pumping scheme with circular symmetry and radial currents. The pumping scheme results in a circularly symmetric condensate with steady-state currents arising from the interplay of spatially nonuniform pumping and decay. We find that the system is dynamically unstable to spontaneous symmetry breaking and undergoes the formation of rotating vortex rings in the absence of any rotating drive or fields. The rings have large net angular momentum and can rotate in either direction. Side bands in the photoluminescence spectrum of the system constitute an experimental signature of such a ring alternative to direct imaging with time-resolved techniques. Due to this and the fact that they dispense with the need for harmonic trapping potentials, they provide great encouragement for the first experimental observation of spontaneous vortex rings in any polariton system. Since the rotation states can be controlled, and are topologically distinct, the system has the potential to find applications in polaritonic devices as a controllable two-state system, or for storing large, definite values of angular momentum that can be used to direct polariton flow.

We thank J. Keeling for helpful discussions. JOH and AKB both acknowledge support from University of Warwick Scholarships. FMM acknowledges financial support from the programs MINECO (MAT2011-22997), and CAM (S-2009/ESP-1503). DS acknowledges the project ERC Polaflow. MHS acknowledges support from EPSRC (EP/I028900/1 and EP/K003623/1).

REFERENCES

- [1] ONSAGER L., *Nuovo Cimento*, **2** (1949) 249.
- [2] LEGGETT A. J., *Quantum liquids: Bose condensation and Cooper pairing in condensed-matter systems* Vol. 34 (Oxford University Press, Oxford) 2006.
- [3] KASPRZAK J. *et al.*, *Nature*, **443** (2006) 409.
- [4] STEVENSON R. M. *et al.*, *Phys. Rev. Lett.*, **85** (2000) 3680.
- [5] BAUMBERG J. J. *et al.*, *Phys. Rev. B*, **62** (2000) R16247.
- [6] WOUTERS M. and CARUSOTTO I., *Phys. Rev. A*, **76** (2007) 043807.
- [7] AMO A. *et al.*, *Nature*, **457** (2009) 291.
- [8] AMO A. *et al.*, *Nature Physics*, **5** (2009) 805.
- [9] SANVITTO D. *et al.*, *Nature Physics*, **6** (2010) 527.
- [10] MARCHETTI F. M., SZYMAŃSKA M. H., TEJEDOR C. and WHITTAKER D. M., *Phys. Rev. Lett.*, **105** (2010) 063902.
- [11] TOSI G. *et al.*, *Phys. Rev. Lett.*, **107** (2011) 036401.
- [12] BORGH M. O., KEELING J. and BERLOFF N. G., *Phys. Rev. B*, **81** (2010) 235302.
- [13] CROSS M. C. and HOHENBERG P. C., *Rev. Mod. Phys.*, **65** (1993) 851.

- [14] TOSI G. *et al.*, *Nature Comms.*, **3** (2012) 1243.
- [15] MANNI F. *et al.*, *Phys. Rev. B*, **88** (2013) 201303.
- [16] HIVET R. *et al.*, *Phys. Rev. B*, **89** (2014) 134501.
- [17] KEELING J. and BERLOFF N. G., *Phys. Rev. Lett.*, **100** (2008) 250401.
- [18] BALILI R. *et al.*, *Science*, **316** (2007) 1007.
- [19] DE GIORGI M. *et al.*, *Phys. Rev. Lett.*, **109** (2012) 266407.
- [20] FRANCHETTI G., BERLOFF N. G. and BAUMBERG J. J., *arXiv preprint arXiv:1210.1187*, (2012) .
- [21] BALLARINI D. *et al.*, *Nature Comms.*, **4** (2013) 1778.
- [22] WHITTAKER D. M., *Phys. Status Solidi*, **2** (2005) 733.
- [23] CARUSOTTO I. and CIUTI C., *Rev. Mod. Phys.*, **85** (2013) 299.
- [24] WHITTAKER D., *Superlattices and Microstruct.*, **41** (2007) 297.
- [25] WHITTAKER D. M., *Phys. Rev. B*, **71** (2005) 115301.
- [26] MARCHETTI F. M. and SZYMAŃSKA M. H., *Vortices in polariton OPO superfluids in Exciton Polaritons in Microcavities*, edited by SANVITTO D. and TIMOFEEV V., (Springer) 2012 pp. 173–213.
- [27] BORGH M. O., FRANCHETTI G., KEELING J. and BERLOFF N. G., *Phys. Rev. B*, **86** (2012) 035307.